medRxiv preprint doi: https://doi.org/10.1101/2020.12.04.20243923; this version posted December 4, 2020. The copyright holder for this preprint (which was not certified by peer review) is the author/funder, who has granted medRxiv a license to display the preprint in perpetuity. It is made available under a CC-BY 4.0 International license .

Correction of human forehead temperature variations measured by non-contact infrared thermometer

Adrian Shajkofci, *Member, IEEE*

***Abstract*— Fever is a common indicator for symptoms of infections, including SARS-CoV-2 or influenza. Non-contact infrared thermometers are able to measure forehead temperature in a timely manner and perform a fast fever screening in a population. However, forehead temperature measurements differ greatly from basal body temperatures and are the target of massive perturbations from the environment. Here we gathered a dataset of N=19392 measurements using the same precision infrared sensor in different locations while tracking both outside temperature, room temperature, time of measurement, and identity. From this, we propose a method able to extract and remove the influence of external perturbations and set a threshold for fever based on local statistics. This method can help manufacturers and decision-makers to build and use more accurate tools so as to maximize both sensitivity and specificity of the screening protocol.**

***Index Terms*— fever, infrared, screening, temperature**

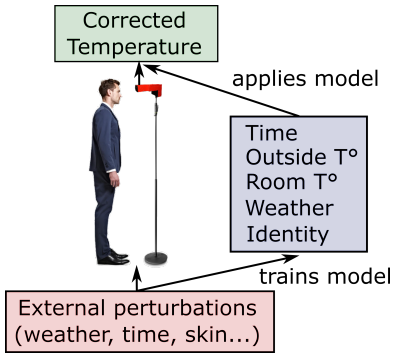

I. Introduction

FEVER, also called pyrexia, is one of the usual clinical features that appears during the course of several infectious diseases, such as influenza or SARS-CoV-2 viral infections. It reduces viral replication and is a straightforward marker of immune response [1]. Body temperature can be measured in numerous ways. The traditional method for such a measurement are contact thermometers placed in the mouth, ear, armpit or rectum. Contact thermometers are measuring temperature using the conduction of heat to a thermocouple, a resistance temperature detector (RTD) or a thermistor through a metallic element. While RTDs are among the most precise temperature sensors available, the process of conduction is slow (around one minute) and the device needs extensive disinfection after use to prevent cross-contamination [2]. Non-contact infrared thermometers (NCITs), on the other hand, allow the temperature to be taken without contact and therefore do not require constant disinfection, take fast measurements (less than one second) and do not require to stay uncomfortably with a thermometer for a long time. Non-contact thermometers were extensively reviewed in [3] and validated for their use for fever symptoms detection.

NCITs can be classified into two categories. Thermal scanners, or thermal cameras are used to take a person temperature from a great distance (in the order of meters), thanks to its cell array. However, they are rather imprecise, with an error of between 0.5 and 5°C compared to contact thermometers. They also are greatly dependent on the fluctuations of air temperature. The second type are thermopiles. They receive the radiant energy released by the object over a constant field of view and convert it into an electrical signal, which is calibrated to the relative temperature of the object. The latter type of thermometer can be accurately calibrated, the ambient air flow being almost negligible since the distance between the sensor and the object is small ($2\,\mathrm{cm}$ to $20\,\mathrm{cm}$). However, even though variations caused by air flow are reduced, many factors affect the temperature measurement of the human body by the skin, such as placement, skin type, moisture, and most importantly, environmental conditions [4]–[6].

In our research, we consider the variation of human forehead temperature in different environments. We then examine if these perturbations influence the measurement accuracy in the context of infection symptom screenings. We believe that the analysis of temperature perturbations on human forehead temperature can be used to improve screening protocols by correcting the perturbations and adapting the fever detection threshold to the variations.

After having described the acquisition modalities in Section II-A, we design a statistical analysis of temperature variation of groups and individuals across time, ambient temperature and meteorological conditions. Then, we propose in Section II-B a method to remove the effect of external perturbations. We publish the results in Section III and conclude in Section IV.

Manuscript received November 17, 2020; revised XXXXXXX XX, XXXX.

Adrian Shajkofci is with the Idiap Research Institute, CH-1920 Martigny, Switzerland and École Polytechnique Fédérale de Lausanne, CH-1015 Lausanne, Switzerland.

NOTE: This preprint reports new research that has not been certified by peer review and should not be used to guide clinical practice.

medRxiv preprint doi: https://doi.org/10.1101/2020.12.04.20243923; this version posted December 4, 2020. The copyright holder for this preprint (which was not certified by peer review) is the author/funder, who has granted medRxiv a license to display the preprint in perpetuity. It is made available under a CC-BY 4.0 International License.

II. Methods

A. Acquisition modalities and sensor calibration

We gathered the data from participating companies that used the infrared sensor module Coronasense (Coronasense, Martigny, Switzerland). The device embeds a thermopile-based sensor element (MLX90614-DCI, Melexis Technologies NV, Belgium) with a reported measurement accuracy of ≤ 0.2°C. The sensor chip is certified to comply with the ASSTM standard section 5.4 (Designation: E1965-98/2009)) - Standard Specification for Infrared Thermometers for Intermittent Determination of Patient Temperature. The devices were installed at the entrance of the buildings and measurements were taken approximately 30 seconds after entrance. For each measurement, the user was told to aim at a point 3 cm above the junction between the eyes, 10 cm away from the sensor. Exact distance between the device and the user was controlled and recorded using a Light Detection And Ranging (LIDAR) detector. A burst of 10 measurements were taken at different positions on the forehead, and the maximal value was kept. For a subset of the data, we gathered an anonymous imprint of the user's identity, so we could track their temperature over time. For another subset of the data, we could also gather the local meteorological conditions at the time of measurement using OpenWeatherMap (OpenWeather Ltd., London, UK).

All sensors were factory calibrated using a black body and automatically calibrated themselves using the temperature of the ambient air. We adjusted the sensor output to the human body emissivity $\epsilon = 0.98$ from Plank's law [7]:

$$T = \sqrt[4]{\frac{T_{amb}^4 - (1-\epsilon)T_{ir}^4}{\epsilon}}, \tag{1}$$

with T_{amb} and T_{ir} the ambient temperature of the environment and the mirrored temperature of the object, respectively. We added to the results an offset of 2.1 degrees in order to match with the average temperature using a contact thermometer, as observed by [3].

B. Correction of environmental perturbations

We now turn to the task of measuring the correlation between the forehead temperature and environmental factors (inside ambient temperature, outside temperature and hours in the days) in the aim of removing the influence of these factors from the raw data. We model the relationship between the forehead temperature and the ambient and outside temperature data as a combination of affine functions $t_a(t) = a_a t + c_a$ and $t_o(t) = a_o t + c_o$ respectively. We also model the relationship between the hours in a day and the forehead temperature as a second degree polynomial function $t_p(t) = t^2 + t + c_p$. We correct the temperature by subtracting to every point of data its corresponding point in the modeled curve or line and multiply, for every environmental perturbation, by the mean of the raw data.

In the same way, one can instead correct the threshold for fever detection by subtracting the offset between the regression curve and the acquired raw data to the fever threshold $t_{\text{max\_corr}}$. For example, to correct the threshold as a function of the outside temperature:

$$t_{\text{max\_corr}}(t) = t_{max} - a_o t - c_o, \tag{2}$$

with a_o and c_o trained from the previous measurements using a least-squares fit.

When it is possible to track measurements of a unique individual over time, we propose a personalized threshold when the temperature measurements can be associated with an individual identifier, computed using the K-th last measurements of the specific person i:

$$t_{\text{max\_corr}}(t^i) = \bar{t^i} + \alpha\sqrt{\frac{\sum^K (\bar{t^i} - t_k^i)^2}{K}}, \tag{3}$$

with $\bar{t^i}$ the mean of K temperature acquisitions for the individual i and $0 < \alpha < 5$ a coefficient for the standard variation. We use $\alpha = 3$ since it is the coefficient so that 99.7% of the data remains detected as healthy under the normal approximation of the temperature distribution curve [8].

In the next section, for illustration purposes, instead of adapting the threshold dynamically for every data point, we adapt the individual temperature values against perturbations with a fixed threshold.

Location	N	Average (°C)	Indiv. deviation (°C)
All	19392	35.38 ± 0.81	0.56 ± 0.28
A	3622	35.57 ± 0.89	0.77 ± 0.24
B	4759	35.30 ± 0.68	N/A
C	2508	35.09 ± 0.69	0.39 ± 0.24

(a) without correction

Location	N	Average (°C)	Indiv. deviation (°C)
All	9839	35.37 ± 0.67	0.49 ± 0.20
A	2966	35.52 ± 0.70	0.57 ± 0.20
B	1539	35.23 ± 0.59	N/A
C	2503	35.3 ± 0.54	0.34 ± 0.19

(b) with corrections

TABLE I: Statistics of the dataset of forehead temperature measurements. We also tracked temperatures of individuals over time and reported the mean of the deviation of temperature for one person over time. The number of measurements after outdoor temperature correction is smaller than without correction due to the availability of meteorological data.

III. Results

A. Population analysis

We measured the temperature of $N = 19392$ during a period of six weeks, in 6 different locations (see Figure 1 (a)) and computed statistics for all locations as well as for individual locations (Table I). We observed an average forehead temperature of 35.38 ± 0.81°C. The average and deviation of these measurements did not change significantly among different locations and populations (see Table I for locations A-C). The distribution of temperatures seem to be skewed toward low temperatures (see Figure 2 (a)).

medRxiv preprint doi: https://doi.org/10.1101/2020.12.04.20243923; this version posted December 4, 2020. The copyright holder for this preprint (which was not certified by peer review) is the author/funder, who has granted medRxiv a license to display the preprint in perpetuity.
It is made available under a CC-BY 4.0 International license.

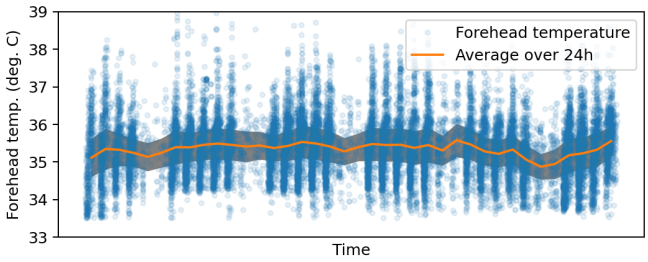

(a) without correction

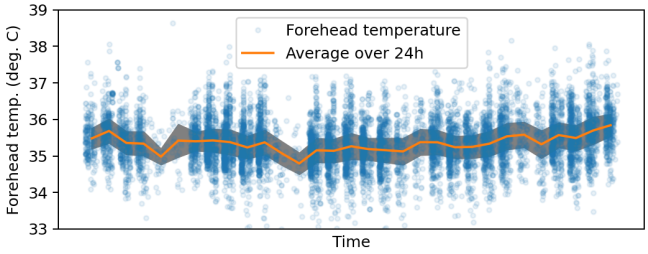

(b) corrected against all perturbations

Fig. 1: Dataset of forhead temperature measurements ($N = 19392$) relatively to time, taken during a period of six weeks. Statistics are shown in Table I. (a) without correction (b) with the corrections computed in Section II-B (ambient, outside and time corrections)

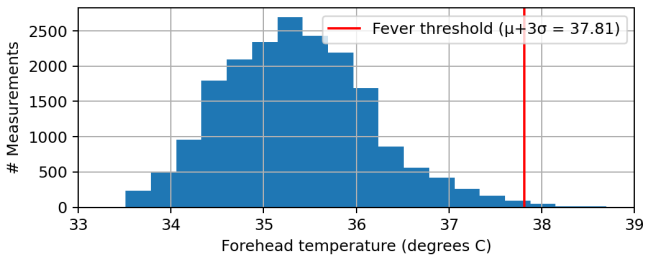

(a) histogram without correction

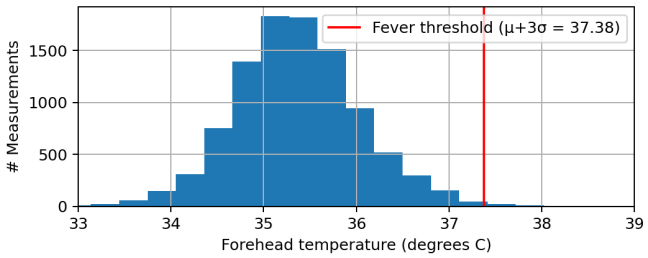

(b) histogram corrected against all perturbations

Fig. 2: Histogram of forhead temperature measurements ($N = 19392$), taken during a period of six weeks. Statistics are shown in Table I. (a) without correction (b) with the corrections computed in Section II-B (ambient, outside and time corrections)

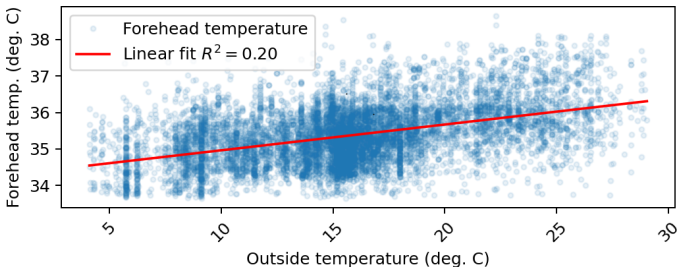

(a) forehead temp. against outside temp. (uncorrected)

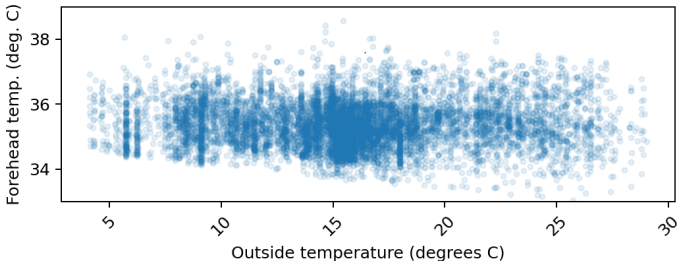

(b) corrected against outside temperature

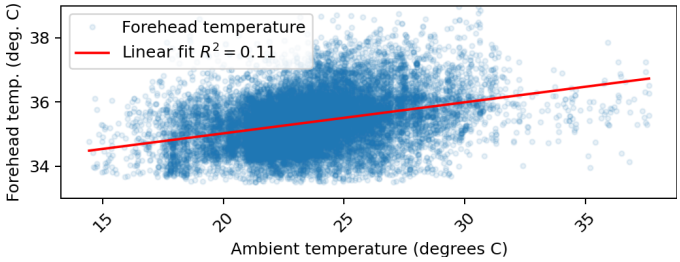

(c) forehead temp. against ambient temp. (uncorrected)

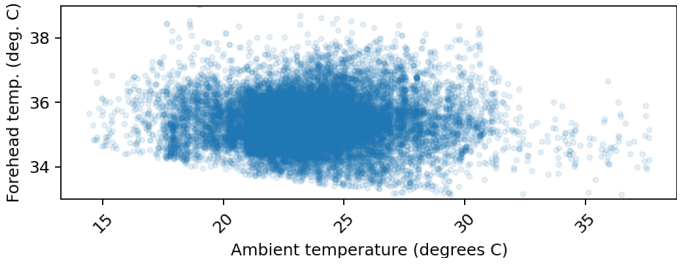

(d) corrected against ambient temperature

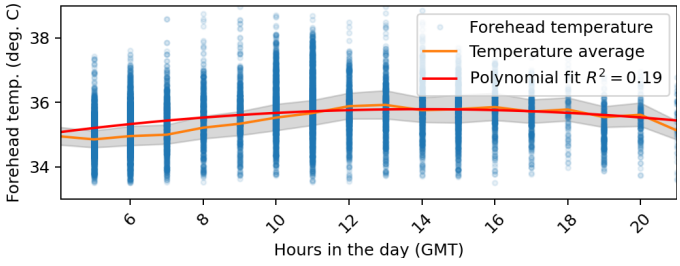

(e) forehead temp. against hours in a day. (uncorrected)

Fig. 3: Dataset of forehead temperature measurements ($N = 19392$) relatively to external perturbations ((a) outside temperature, (c) room temperature, (e) hour of measurement), taken during a period of six weeks, before and after correction for environmental effects. The number of measurements after outdoor temperature correction is smaller than without correction due to the availability of meteorological data.

medRxiv preprint doi: https://doi.org/10.1101/2020.12.04.20243923; this version posted December 4, 2020. The copyright holder for this preprint (which was not certified by peer review) is the author/funder, who has granted medRxiv a license to display the preprint in perpetuity. It is made available under a CC-BY 4.0 International License.

B. Tracking of individual temperature data

After having looked at the data from an ensemble point of view, we now turn to the tracking of temperatures of individuals over time. For a subset of the data ($N = 12882$), we were able to gather individual anonymous tagging for every temperature measurement, along with all other features already analyzed in Section III-A. Results shown in Table I for variations of temperature of an individual over time indicates that the individual variation (0.56 ± 0.28°C) was lower than the average variation of temperature in a population (0.81°C).

C. Correction of environmental perturbations

We were able to retrieve, on a subset of the dataset ($N = 9839$), the meteorological data of the exact measurement location at the time when the measurement was taken. We then trained the regression models from Section II-B. There was a significant correlation between outside temperature ($R^2 = 0.20$) and forehead temperature in terms of Pearson correlation coefficient. Room temperature had a lower influence on the data ($R^2 = 0.11$), since some measurements were taken when the individual entered a particular building. A similar correlation ($R^2 = 0.19$) was found by comparing the measurements with their acquisition times within a 24-hour day. From the trained regression curves, we were able to subtract the differences representing the coupling of features for ambient, outside temperature and time of the day with the forehead temperature ($R^2 = 0$) (see Figure 1 (b)). After correction, the variation of temperatures across both population and time were reduced (Table I (b)) and the histogram of temperature density appeared to follow a Gaussian curve (Figure 2 (b)).

IV. Conclusions

Thanks to the data analyzed in this study, we found out that the average forehead temperature was 35.38 ± 0.81 °C. This number was consistent across different places and matched to the values found in [9], [10], after proper scaling. Similarly to [3], we propose a fever detection temperature threshold of the mean plus 3 times the standard deviation of the temperatures in our dataset (37.81 with the offset we applied, or 35.68°C without calibration). After correction of external components, this threshold is reduced to 37.38°C, which is consistent with the new data from [8]. Using the same calculation, this threshold could even be lowered due to the smaller deviation of measurements in specific environments (see Table I for Location B-C).

We modeled the relationship between outside, ambient temperatures, hours in the day and the measured forehead temperature as first and second degrees polynomials. Using these models, we were able to subtract the influence of external perturbations and drastically reduce the co-linearity between these features. Such correlations between perturbations and the measured forehead temperature reveals that corrections to the temperature or fever detection threshold can lead to a better detection accuracy of high temperature symptoms.

Furthermore, we found that the deviation of the forehead temperature of one individual over time is lower than the deviation of the mean temperature in a population. These findings confirm the idea that every individual is biologically distinct in terms of temperature and skin type due to demographic and physiological factors [11]. Consequently, the limit threshold for fever might be individual as well. Personalized thresholds and tracking may then have a significant advantage over static thresholds for fever screening, since the personalized threshold may be lower than the global threshold.

In a time when disease outbreaks can spread worldwide very easily and at high speeds, fast disease screening solutions, such as fever screening, appear to be necessary. We hope that this research helps decision-takers and manufacturers to build more robust and intelligent tools that use multi-dimensional data in order to maximize both sensitivity and specificity of the screening protocol.

V. Declarations

Code and datasets will be available online (github) upon acceptance. AS work for Coronasense, Martigny, Switzerland, who gathered and released the raw data.

VI. References

[1] M. Yamaya *et al.*, "Effects of high temperature on pandemic and seasonal human influenza viral replication and infection-induced damage in primary human tracheal epithelial cell cultures," *Heliyon*, vol. 5, no. 2, 2019.

[2] V. Betta, F. Cascetta, and D. Sepe, "An assessment of infrared tympanic thermometers for body temperature measurement," *Physiol Meas*, vol. 18, no. 3, pp. 215–225, 1997.

[3] H.-Y. Chen, A. Chen, and C. Chen, "Investigation of the Impact of Infrared Sensors on Core Body Temperature Monitoring by Comparing Measurement Sites," *Sensors (Basel)*, vol. 20, no. 10, 2020.

[4] M. S. Ganio *et al.*, "Validity and Reliability of Devices That Assess Body Temperature During Indoor Exercise in the Heat," *J Athl Train*, vol. 44, no. 2, pp. 124–135, 2009.

[5] C. B. Mogensen *et al.*, "Forehead or ear temperature measurement cannot replace rectal measurements, except for screening purposes," *BMC Pediatrics*, vol. 18, no. 1, p. 15, 2018.

[6] A. Dante *et al.*, "Evaluating the Interchangeability of Forehead, Tympanic, and Axillary Thermometers in Italian Paediatric Clinical Settings: Results of a Multicentre Observational Study," *Journal of Pediatric Nursing*, vol. 52, e21–e25, 2020.

[7] V. Bernard *et al.*, "Infrared camera assessment of skin surface temperature – Effect of emissivity," *Physica Medica*, vol. 29, no. 6, pp. 583–591, 2013.

[8] J. S. Hausmann *et al.*, "Using Smartphone Crowdsourcing to Redefine Normal and Febrile Temperatures in Adults: Results from the Feverprints Study," *J GEN INTERN MED*, vol. 33, no. 12, pp. 2046–2047, 2018.

medRxiv preprint doi: https://doi.org/10.1101/2020.12.04.20243923; this version posted December 4, 2020. The copyright holder for this preprint (which was not certified by peer review) is the author/funder, who has granted medRxiv a license to display the preprint in perpetuity.
It is made available under a CC-BY 4.0 International license.

[9] D. K.-k. Ng *et al.*, "A brief report on the normal range of forehead temperature as determined by noncontact, handheld, infrared thermometer," *Am J Infect Control*, vol. 33, no. 4, pp. 227–229, 2005.

[10] H. Apa *et al.*, "Clinical accuracy of tympanic thermometer and noncontact infrared skin thermometer in pediatric practice: An alternative for axillary digital thermometer," *Pediatr Emerg Care*, vol. 29, no. 9, pp. 992–997, 2013.

[11] Z. Obermeyer, J. K. Samra, and S. Mullainathan, "Individual differences in normal body temperature: Longitudinal big data analysis of patient records," *BMJ*, vol. 359, 2017.